J Biomol NMR (2011) 49:185–193
DOI 10.1007/s10858-011-9486-4

ARTICLE

^{1}H NMR metabolomics identification of markers of hypoxia-induced metabolic shifts in a breast cancer model system

Aalim M. Weljie · Alla Bondareva · Ping Zang · Frank R. Jirik

Received: 22 October 2010 / Accepted: 15 December 2010 / Published online: 4 March 2011

Abstract Hypoxia can promote invasive behavior in cancer cells and alters the response to therapeutic intervention as a result of changes in the expression many genes, including genes involved in intermediary metabolism. Although metabolomics technologies are capable of simultaneously measuring a wide range of metabolites in an untargeted manner, these methods have been relatively under utilized in the study of cancer cell responses to hypoxia. Thus, ^{1}H NMR metabolomics was used to examine the effects of hypoxia in the MDA-MB-231 human breast cancer cell line, both in vitro and in vivo. Cell cultures were compared with respect to their metabolic responses during growth under either hypoxic (1% O_2) or normoxic conditions. Orthogonal partial least squares discriminant analysis (OPLS-DA) was used to identify a set of metabolites that were responsive to hypoxia. Via intracardiac administration, MDA-MB-231 cells were also used to generate widespread metastatic disease in immunocompromised mice. Serum metabolite analysis was conducted to compare animals with and without a large tumor burden. Intriguingly, using a cross-plot of the OPLS loadings, both the in vitro and in vivo samples yielded a subset of metabolites that were significantly altered by hypoxia. These included primarily energy metabolites and amino acids, indicative of known alterations in energy metabolism, and possibly protein synthesis or catabolism. The results suggest that the metabolite pattern identified might prove useful as a marker for intra-tumoral hypoxia.

Keywords Metabolomics · ^{1}H NMR spectroscopy · Hypoxia · Glycolysis · Breast cancer · Chemometrics · OPLS-DA · Tumor xenograft

Abbreviations

HIF	Hypoxia inducible factor
MCT	Monocarboxylate transporter
MDA-MB-231-Luc2	MDA-MB-231 Luciferase
OPLS-DA	Orthogonal partial least squares discriminant analysis
PCA	Principal component analysis
VIP	Variable influence on projection

A. M. Weljie (✉)
Department of Biological Sciences, University of Calgary, 2500 University Dr. NW, Calgary, AB T2N 1N4, Canada
e-mail: aweljie@ucalgary.ca

A. Bondareva · F. R. Jirik
Department of Biochemistry and Molecular Biology, McCaig Institute for Bone and Joint Health, Calgary, AB, Canada

Present Address:
A. Bondareva
Department of Comparative Biology and Experimental Medicine, Calgary, AB, Canada

Present Address:
P. Zang
Department of Chemistry, University of Calgary, Calgary, AB T2N 1N4, Canada

Introduction

Tumor progression is accompanied by number of metabolic events, some of which facilitate the processes of tumor invasion and metastasis to distant organs. One well established metabolic phenomenon is the abnormal induction of glycolysis occurring under either aerobic or anaerobic conditions. The former was made famous by Otto Warburg, and hence has been referred to as the 'Warburg

effect' (Warburg 1956). In this case, there is a down-regulation of oxidative phosphorylation, and an up-regulation of processes that are typically observed in cells grown under conditions of reduced oxygen tension. Of particular note is the up-regulation of the transcription factor, hypoxia-inducibile factor-1α (HIF-1α), that triggers a number of protective and pro-invasive events in tumor cells (DeBerardinis et al. 2008). There are indications that a number of complex phenomena that occur in addition to the Warburg effect play key roles in hypoxia-mediated events (recently reviewed in (Weljie and Jirik 2010)).

The various metabolic perturbations seen in cancers suggest the possibility of identifying tumor-associated metabolites that could prove of value in following the course of this disease. For example, there have been reports of hypoxia-related metabolites in tumors, although primarily in a pathway-specific manner. Thus, studying the effects of HIF-1β, Griffith and colleagues used ^{13}P MRS and ^{1}H NMR to examine phosphorylated nucleotide (NTP)-related metabolites, making the surprising finding of significant decreases in the absolute concentrations of ATP, but not the ratio of NTP/phosphate ratio (Griffiths et al. 2002). Another example of targeted metabolite flux analysis, using hypoxic glioma cells, employed the addition of ^{13}C-glucose and ^{13}-pyruvate to the cell culture media, and demonstrated a central role for pyruvate under hypoxic conditions (Perrin et al. 2002).

The effects of hypoxia in cancer have been less well studied by broad-based metabolite profiling methods, commonly referred to as 'metabolomics' studies. This approach is particularly important to the search for biomarkers that can be detected within clinically accessible fluids such as urine or serum. For such applications, we have found ^{1}H NMR to be a valuable tool owing to the quantitative (Weljie et al. 2006) and reproducible (Lindon et al. 2003) nature of NMR profiling. These two advantages are further enhanced by the application of sophisticated post-processing tools such as 'targeted profiling' that allow for a quantitative library-based data-reduction of an NMR spectrum into its latent metabolites (Weljie et al. 2006; Chang et al. 2007), or unknown peaks (Weljie et al. 2008). Our group has pioneered the use of these tools for analysis of complex bio-fluid spectra, as was used in a study of serum derived from a murine inflammatory arthritis model (Weljie et al. 2007).

In the current study, we set out to search for biologically relevant biomarkers of hypoxia in cancer cells by examining the relationship between metabolites altered in a cell culture model of MDA-MB-231 breast cancer cells, and in serum from mice with multiple metastases derived from these cells. Examination of the extracellular metabolome for cell studies has been referred to as the metabolic 'footprint', and previously studied, for example, in yeast (Allen et al. 2003), and plants (Dowlatabadi et al. 2009), and has also been applied to breast cancer cells (Claudino et al. 2007). Using quantitative NMR metabolomics methods and orthogonal partial least squares discriminant analysis (OPLS-DA) chemometric methods, we have identified a subset of metabolites common to both the in vivo and in vitro models. Although other tumor models would need to be examined, the metabolite pattern described herein has the potential of serving as a useful biomarker of solid tumor hypoxia.

Materials and methods

Cell growth

A derivative of the human breast cancer cell line MDA-MB-231 (kindly provided by Dr. T. Guise, Vanderbilt University) that we generated (Bondareva et al. 2009), designated MDA-MB-231-Luc2, was plated at low density and incubated either in ambient, or 1% oxygen (using a triple-gas incubator), and 5% CO_2 at 37°C. Culture medium was DMEM (Invitrogen), supplemented with 1× Serum Replacement I (Sigma) and 1% penicillin/streptomycin, and cells were grown until they reached 100% confluency. Medium in the confluent plates was then replaced with fresh medium that had been pre-equilibrated to the specific oxygen conditions, with the day of medium replacement being considered as day "0". Aliquots of the medium were then collected every day during the incubation of cells. After the 3 days of the incubation the medium was collected and replaced completely with fresh pre-equilibrated medium to ensure adequate nutrient availability throughout the course of the experiment. Cell viability, evaluated by trypan blue staining at the end of the 5-days period of incubation, was >95% for both the normoxic and hypoxic groups. Cells were harvested at either day 3 or 5, collected as cell pellets containing 1.2×10^7 cells per sample, and stored at −80°C until ready for analysis.

In vivo metastasis model

To generate metastases, 5–6 week old female NIH-III (*nu/nu; beige/beige*) mice (Charles River Laboratories, St-Constant, QC) were anesthetized by intraperitoneal (i.p.) injection of ketamine (100 mg/kg) and xylazine (6 mg/kg), and 2×10^5 MDA-MB-231 cells stably expressing firefly luciferase (MDA-MB-231-Luc2) suspended in 100 µL of PBS were injected into the left ventricle of each mouse as previously described (Bondareva et al. 2009). Mice were housed under viral antibody-free conditions in the biohazard area of the University of Calgary Animal Resources

Center in compliance with Canadian Council of Animal Care guidelines and with ethical approval from the University of Calgary Animal Care Committee. Food and water was given *ad libitum*. Development of metastases was monitored via bi-weekly bioluminescence imaging as described elsewhere (Bondareva et al. 2009). Briefly, the mice were administered *D*-luciferin (Gold Bio Technology; St. Louis, MO), at a dose of 150 mg/kg in PBS by i.p. injection, and anesthetized with 1.5–2% isofluorane for 10–12 min prior to imaging. Mice were then placed onto the warmed stage inside of the light-tight box of a Xenogen IVIS Lumina system (Caliper Life Sciences) and imaged in both the dorsal and ventral positions. Imaging parameters were f/stop 1, bin 4, field of view 12.5 cm, and exposure times ranged from 20 s to 2 min, depending on the strength of tumor photon emission rates. Results were analyzed using Living Image 3.0 software (Caliper Life Sciences). Signal intensity was quantified as the total photons/s of the whole body image with the background bioluminescence subtracted out. Mice were sacrificed 21 days after the MDA-MB-231-Luc2 cell injections, and blood samples were collected via cardiac puncture. The blood was allowed to clot for 10 min at room temperature. The clotted material was removed by centrifugation at 10,000 rpm for 10 min. Hemolysis was not observed. Serum obtained from the blood samples was frozen immediately and stored at −80°C. Micro-computed tomography (μCT) of the femora/tibia was performed as described previously (Bondareva et al. 2009) using a μCT40 instrument (Scanco Medical, Brüttisellen, Switzerland).

Sample preparation and NMR spectroscopy

All samples from in vitro culture and serum samples were prepared using an ultrafiltration protocol as previously described (Weljie et al. 2007). Briefly, serum (~200 μL) or supernatants (300 μL) were filtered using a 2 mL, 3 kDa membrane centrifuge filter (Pall) after washing to remove preservative compounds. The filter was washed with 50 μL D_2O and all flow-through collected and buffered to 100 mM Na_2HPO_4/NaH_2PO_4, pH 7.00 ± 0.05. DSS (4,4-dimethyl-4-silapentane-1-sulfonic acid) as an internal standard, 0.5 mM, and 0.02% $NaNa_3$ added as a preservative in a final volume of 650 μL. NMR spectroscopy was conducted on a Bruker Avance II 600 spectrometer with a proton frequency of 600.22 MHz with a TXI probe (5 mm) at a temperature of 298°K. One-dimensional experiments used a standard 1D-NOESY pulse sequence (noesypr1d) with irradiation of the water peak during the relaxation delay (1 s) and mixing time (100 ms). Spectra were acquired with 64 K datapoints and a sweepwidth of 12,195 Hz, with 512 transients and a total recycle delay of 5 s. Spectra were processed in a standardized manner using Chenomx NMR Suite v. 4.6 (Chenomx Inc, Edmonton, Canada) with 0.2 Hz line-broadening, Fourier-transformation, phasing and baseline correction. 2-D spectra were acquired in order to confirm identification of the metabolites using ^{1}H- and ^{13}C-chemical shifts compared to those in the HMDB (Wishart et al. 2007), including ^{1}H-^{1}H-TOCSY and ^{1}H-^{13}C HSQC. Proton spectra were quantified using the 'Targeted Profiling' approach (Weljie et al. 2006), as implemented in the Chenomx Software.

Statistical analysis

Metabolite concentrations were exported from the Chenomx software and imported directly into SIMCA-P (Umetrics, Umeå, Sweden). Concentrations were mean-centered and scaled to unit-variance and a per-metabolite basis prior to pattern recognition analysis. Prinicipal component analysis (PCA) was conducted on all data sets initially to evaluate overall patterns and check for outliers.

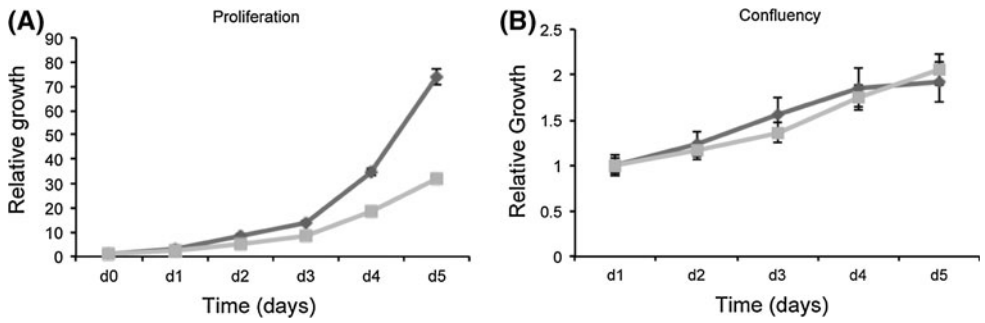

Fig. 1 Cultures of MDA-MB-231-Luc2 cells growth in either ambient oxygen or 1% oxygen. **a** Shows the proliferation of cells plated at 40 cells/mm^2 and grown under normoxic (*black diamonds*) and hypoxic (*grey squares*) conditions. **b** Cells were plated at confluency and then maintained in culture for a period of 5 days. Medium was replaced on Day 3. The data shows that cell numbers were equivalent under the two experimental conditions when cells were growing at near-confluency. Viability at all time points was >95%

Subsequently, supervised regression analysis was conducted using orthogonal partial least squares discriminant analysis for model interpretation. The supervising Y-variable consisted either of day of sampling (cell culture experiments), or a binary hypoxia or normoxia growth status (cell cultures) or binary tumor or control status (mouse model). Metabolites with higher than average significance on each supervised model were evaluated using the variable influence on projection (VIP) parameter. VIP values ≥ 1 within a 95% were considered significant for biological interpretation. Univariate significance testing was conducted in gnu R (www.R-project.org) using a unpaired, two-sided, Welch two sample student *t*-test.

Results

In vitro cell culture experiments

In order to determine the effect of hypoxia on growth of tumor cells, we examined the effect of low oxygen (1% O_2) on the growth of MBA-MB-231-Luc2 cells. Hypoxia led to a slowed growth rate ($\sim$50% reduction) as compared to growth under normoxic conditions as demonstrated by cell counts obtained over a 5 days period of growth of cells initially plated at equivalent numbers (Fig. 1a). In order to ensure that subsequent analyses were reflective of metabolic differences related to culture conditions as opposed to media nutrient depletion resulting from rapid cell growth, the cultures were normalized so that they reached equivalent levels of confluency by day 5 (Fig. 1b).

Metabolomics analysis of cell cultures

Supernatants from the cell cultures were sampled initially when the fresh media (O_2 condition equilibrated) was added to the cultures, and the again daily for 5 days ($T = 0, 1, 2, 3, 4, 5$). Sample processing, NMR spectroscopy and targeted profiling analysis were conducted as described in the methods, with a total of 69 metabolites considered for quantitative analysis. The scores plot from multivariate pattern recognition using PCA is shown in Fig. 2a. In this analysis, the extracellular metabolite pools are visibly distinct between the cells grown under hypoxic and normoxic conditions. The metabolic trajectory (denoted by the lines between the various time points) is somewhat similar, but there is a clear difference in the direction. Cells grown under both hypoxic or normoxic conditions demonstrated a modest retrograde shift between days 3 and 4 which was due to tissue culture medium replenishment. Interestingly, the main difference in the orthogonal component (*y*-axis of Fig. 2b) was related primarily to the hypoxic growth. As a result, another supervised OPLS-DA model was built in which the growth condition (i.e. the O_2 level) was used as the supervisory variable (Fig. 2c). This model was subsequently used for further interpretation of metabolite responses.

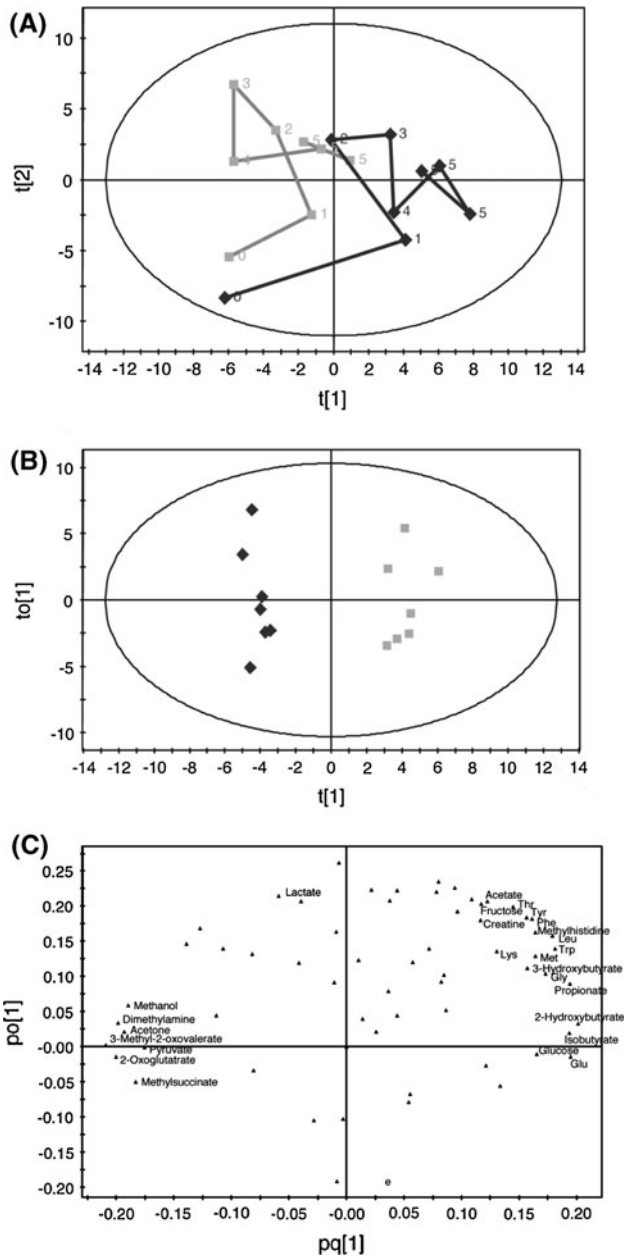

Fig. 2 Multivariate analysis of ^{1}H NMR metabolomics data from supernatants of cell cultures. **a** Scores plot from PCA analysis. Each point represents a single cell supernatant, and the day of collection is labeled. Each day is connected by a line to form a metabolic trajectory during the collection. ($R^2 = 0.656$, $Q^2 = 0.332$). **b** Scores plot from the OPLS-DA analysis of the same samples, with the hypoxia/normoxia status used as the supervisory variable. ($R^2 = 0.969$, $Q^2 = 0.901$, $p = 1.5e^{-4}$). **c** Loadings plot from the OPLS-DA analysis, with the most influential metabolites labeled (VIP $\geq$ 1)

Xenograft model of metastatic breast cancer

MDA-MB-231 cells readily generate systemic metastases when introduced into NIH-III mice via the intra-cardiac route. Figure 3a demonstrates how tumor growth can be readily assessed by bioluminescence imaging owing to luciferase present within the MDA-MB-231-Luc2 cells. The most common site of metastasis is bone, as shown by a representative μCT-scan exhibiting massive osteolytic damage in the distal femur as well as the proximal tibia of a mouse knee (Fig. 3b). As shown in Fig. 3c, tumor growth was exponential, with total tumor burdens (as reflected by whole-mouse photon emission rates) being relatively constant across the panel of animals from which serum was sampled at day 21. Depending on the detection scale selected, anatomical sites with the largest tumors lead to the highest photon emission rates (represented by the red coloration), and by day 21 significant levels of metastatic disease were evident. Large MDA-MB-231-Luc2 metastases, such as we see in the mice, have been shown to have necrotic and/or ischemic regions within them (Erler et al. 2006; Erler et al. 2006).

Metabolomics analysis of mouse serum

Metabolites within the mouse serum were quantified in the same manner as described for the cell culture supernatants. Figure 4a depicts the PCA scores plot of serum from mice with and without tumors. There was significant separation of the two groups, indicating that a substantial metabolic imprint of the tumor was evident in the circulation. A subsequent OPLS-DA analysis (Fig. 4b) was used to ensure that the variance in metabolites related to the tumor growth was rotated into the primary component (t[1]) in order to allow for a comparison of specific metabolites altered under hypoxic cell culture conditions. The loadings plot from the OPLS-DA analysis is shown in Fig. 4c, with the most influential variables highlighted (VIP $\geq$ 1).

Comparison of in vitro and in vivo studies

In order to compare the specific metabolites that were altered between the MDA-MB-231-Luc2 cells grown under hypoxic conditions and the serum from animals with metastases, a two step-filtration process was used. First, the most influential metabolites from both models were selected based on the criteria of VIP $\geq$ 1 in the respective OPLS-DA models. Subsequently, these were compared, and only metabolites that were significant in both models retained. This final set of metabolites is presented in Fig. 5a which as a cross-plot of the loadings values for these compounds from the two OPLS-DA models. This representation draws inspiration from previously published shared and unique structure plots (SUS) (Wiklund et al. 2008). Metabolites with similar coefficients from the modeling process appear on the diagonal of this plot. The

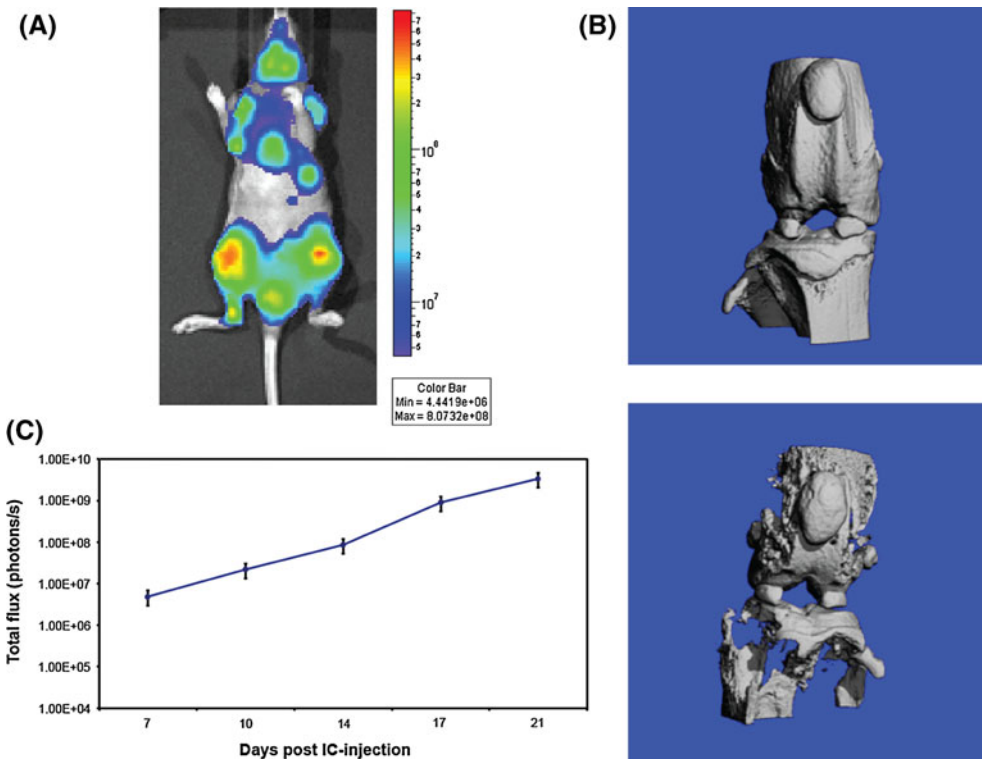

Fig. 3 Imaging of MDA-MB-231-Luc2 metastatic tumors in a representative NIH-III mouse. **a** Ventral view of the mouse with typical pattern of metastases at 21 days following intracardiac injection of MDA-MB-231-Luc2 cells. Each animal had multiple metastases, primarily in bones, but also various internal organs. *Color bar* reflects the photon emission rates from the different metastatic sites (photons/cm^2) following luciferin administration. **b** μCT images of the knees of normal (*upper panel*) and xenografted (*lower panel*) mice, with the latter showing severe osteolytic damage in both the distal femur and proximal tibia. **c** Time course of total body light emission from NIH-III mice carrying MDA-MB-231-Luc2 metastases (log scale, $n = 10$)

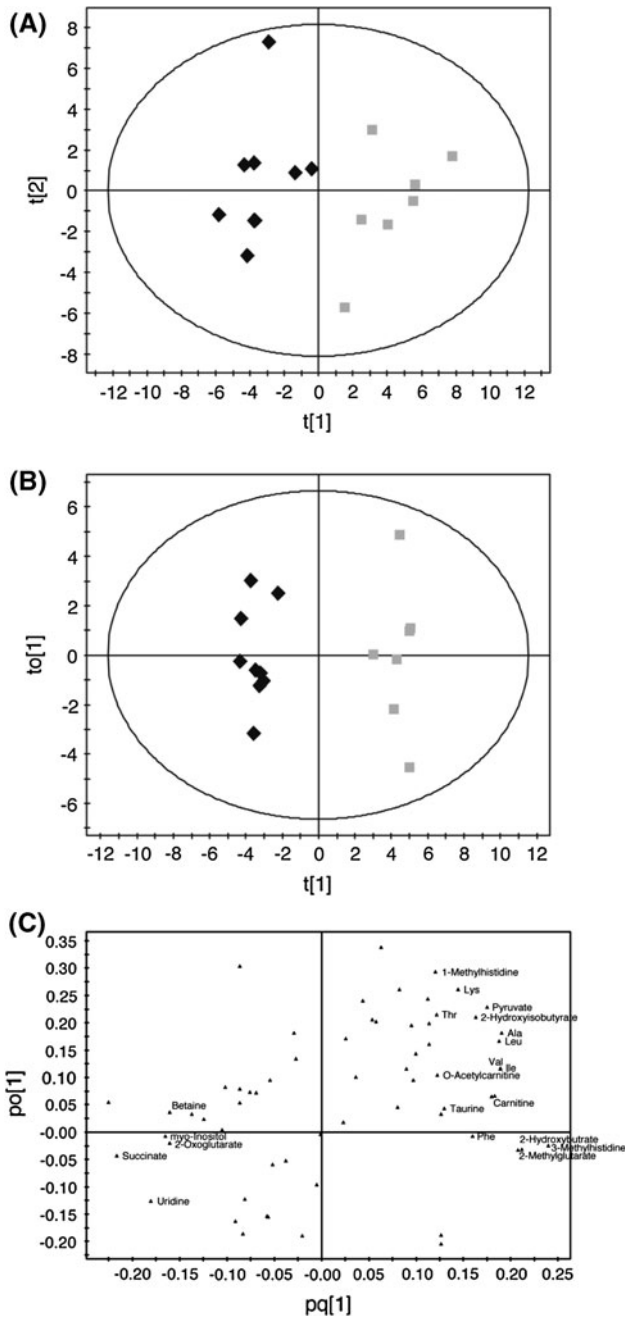

Fig. 4 Multivariate analysis of ^{1}H NMR metabolomics data from serum of NIH-III mouse with metastatic MDA-MB-231-Luc2 xenograft tumors after 21 days. **a** Scores plot from PCA analysis. Each point represents a single serum sample. ($R^2 = 0.424$, $Q^2 = 0.091$). **b** Scores plot from the OPLS-DA analysis of the same samples, with the hypoxia/normoxia status used as the supervisory variable. ($R^2 = 0.974$, $Q^2 = 0.876$, $p = 6.4e^{-5}$). **c** Loadings plot from the OPLS-DA analysis, with the most influential metabolites labeled (VIP $\geq$ 1)

majority of compounds are close to the diagonal, indicating that higher concentrations in animals with tumors correlates with elevated levels in hypoxic cell cultures. The notable exception to this relationship was observed for pyruvate, which was elevated in the serum of animals with tumors (relative to control animals), but reduced in the hypoxic cell cultures (relative to cells grown under normoxia). The specific levels of each one of these metabolites is further described in Fig. 6, along with the univariate significance.

One of the notable features of the hypoxia-specific markers we identified was the absence of lactate, a metabolite regarded as one of the key products of anaerobic metabolism. The VIP scores for lactate indicate that although it was reasonably influential in the murine metastasis model analysis (VIP = 0.944), it was completely non-influential in the cell culture analysis (VIP = 0.363). The concentrations of lactate determined by NMR in both the serum samples from mice with tumors and cell cultures is shown in the last panel of Fig. 6.

Discussion

A key question in translational research, and in particular biomarker discovery, lies in the applicability of in vitro analyses to 'real life' human clinical scenarios. In this study, we have taken an intermediate approach by comparing the in vitro responses of hypoxic tumor cells to the responses of mice bearing well-characterized xenograft tumor model replicating many of the features of the tumor-host interaction that occur in human breast cancer. It is notable that we did find a degree of overlap between metabolites from the in vitro and in vivo studies, and the results are much stronger than would be expected by chance alone.

Metabolite markers of hypoxia

The majority of markers similarly regulated between the cell supernatants and the serum samples, were increased in the cell supernatants in response to hypoxia. This included the amino acids Leu, Thr, Lys, Phe, 1-methylhistidine, as well as 2-hydroxybutrate (2HB). 2HB is a downstream product of (i) amino acid catabolism (Thr, Met and homoserine) and (ii) glutathionine anabolism (Landaas 1975). The increase in Thr observed is consistent with this observation. The amino acids themselves may be present at higher levels due to a number of possible mechanisms, including decreased protein synthesis due to hypoxia, and possibly as a result of HIF-1 mediated induction of autophagy (Wouters and Koritzinsky 2008; Zhang et al. 2008).

The lone metabolite whose concentration was reduced across both experiments was 2-oxoglutarate (2OG). 2OG is a key metabolite in the citric acid cycle of oxidative phosphorylation in mitochondria, a process that is reduced under hypoxic conditions, but also as a result of altered

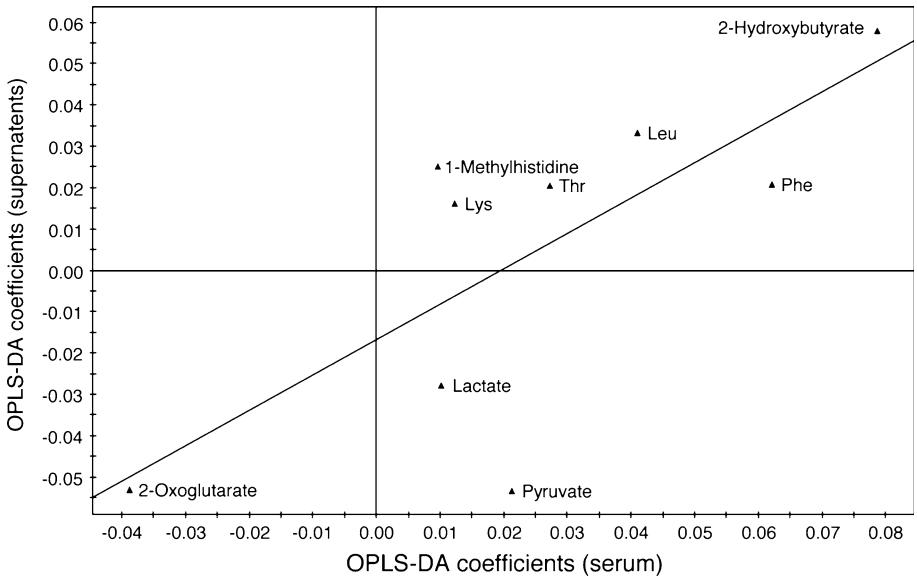

Fig. 5 Cross-plot of the OPLS-DA coefficients for metabolites significant in both the mouse xenograft model (*x*-axis) and cell culture model (*y*-axis). *Positive values* indicate relative increases in metabolite concentrations in animals with tumors and cells grown under hypoxic conditions, respectively. *Diagonal line* indicates best fit line for the two sets of coefficients ($R^2 = 0.538$)

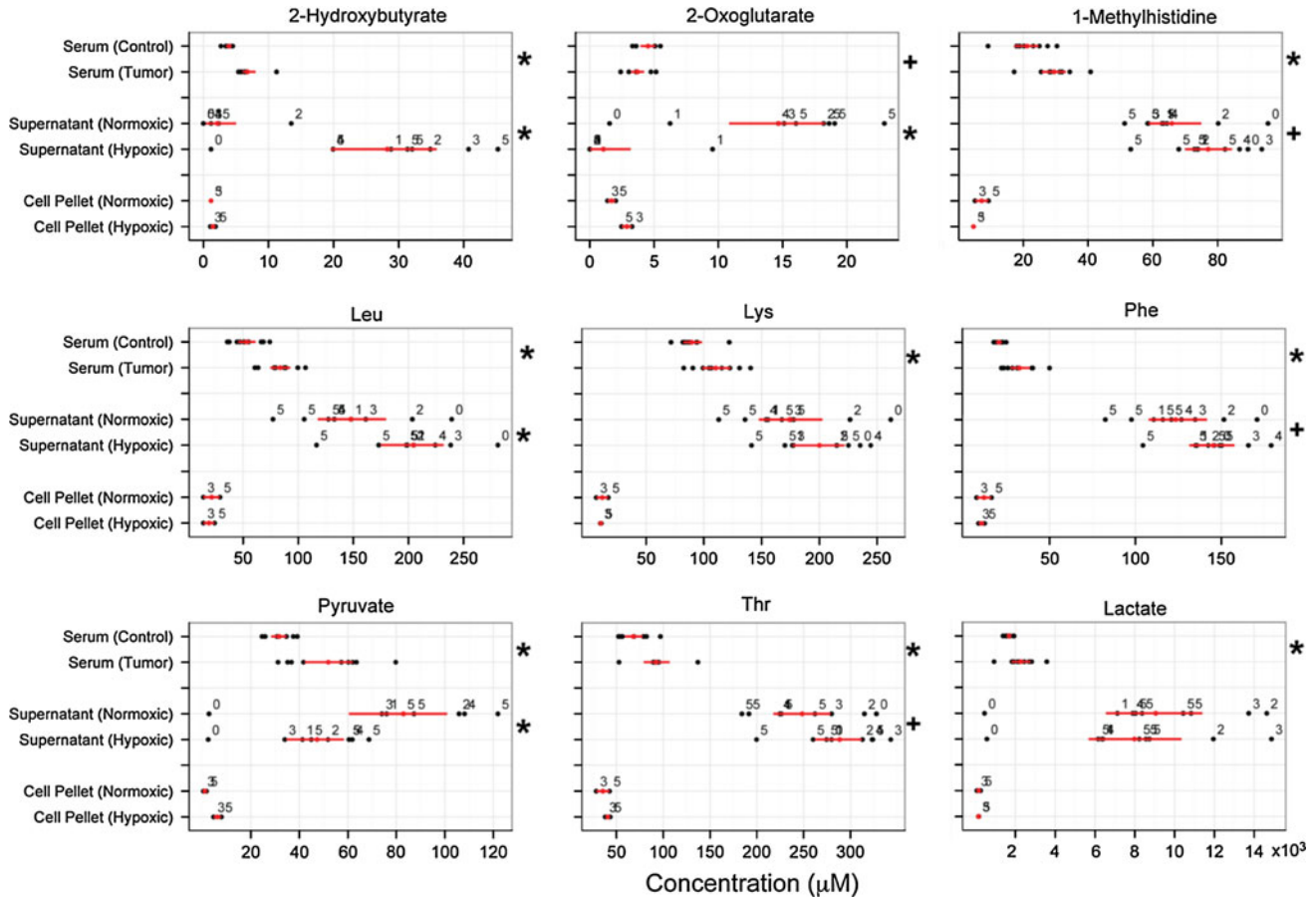

Fig. 6 Metabolite concentrations determined by targeted profiling for all metabolites with significance in both the in vitro and in vivo multivariate modeling, as well as lactate. Determined concentration for each sample is plotted (*black dot*), as well as the mean value (*red dot*) and 95% confidence interval of the mean (*red line*). Time of sampling (in days) is denoted by the numbers on the cell culture values. Univariate significance is denoted in the right hand margin (+, $p < 0.1$; *, $p < 0.05$)

HIF-1-regulation during aerobic glycolysis. Furthermore, 2-oxoglutarate-dependent dioxygenases are an important part of oxygen-sensing mechanisms that regulate HIF-1 activity (Schofield and Ratcliffe 2004; Webb et al. 2009).

Lactate and pyruvate

Two of the more intriguing findings from the study were that (i) pyruvate was significantly altered both in vitro and in vivo, but in an inverse manner, and (ii) lactate was not significantly different in the cell culture media under hypoxic conditions. ^{13}C labeling experiments on cells grown under hypoxic conditions have demonstrated an increased conversion of ^{13}C pyruvate to ^{13}C lactate compared to normoxic growth in rat glioma C6 and human hepatoblastoma HepG2 cells (Perrin et al. 2002). This hypoxia-driven reaction is mediated via pyruvate dehydrogenase kinase-1 (PDK-1), and has been associated with poor prognosis in head and neck cancers (Wigfield et al. 2008). PDK1 is a mitochondrial matrix regulatory enzyme of the pyruvate dehydrogenase (PDH) complex. PDH converts pyruvate to Acetyl-CoA, and phosphorylation of PDH by PDK inactivates PDH.

The pyruvate—lactate relationship is likely central to the differences observed in the concentrations of both metabolites in our in vitro and in vivo studies. Flux of extracellular lactate through monocarboxylate transporters 1 and 4 (MCT1/4) may drive conversion of pyruvate to lactate, and hence lead to lower concentrations in culture supernantants. It has been demonstrated that MCT4 is upregulated in a HIF-1α-dependent manner, leading to increased lactate efflux under hypoxic conditions in Hela, COS, and HL-1 cells (Ullah et al. 2006). This result, combined with results from the ^{13}C pyruvate labeling experiments described above suggests an extracellular increase in lactate levels. However, recent work suggests that this increase may be offset under aerobic conditions, as lactate can be taken up by cells via MCT1 for further metabolism in SiHa cervical cancer cells, but not WiDr colorectal cancer cells (Sonveaux et al. 2008). A confounding factor in these experiments resides in the definition of 'hypoxia' and the responsiveness of a given cell line to hypoxia; for example, our study employed 1% O_2, while other studies have used O_2 levels ranging from 0.1 to 3%. It is possible that in our experiments of the net MCT1/MCT4 activity in the cell cultures resulted in different levels of lactate and pyruvate. Also, there are clear difference in lactate metabolism between different cell lines, making general conclusions about hypoxic lactate metabolism of cell cultures difficult. It should be noted that the levels of lactate in the serum of animals with metastatic tumors was elevated, consistent with model studies of energy metabolite gradients (Walenta et al. 2001).

Model system considerations

One of the advantages of this study was our ability to examine metabolite responses in vivo, and then to extract out those components that were likely due to hypoxia away from those stemming from other metabolic processes. Especially since animals with tumors may exhibit diverse changes in metabolism due to factors other than hypoxia, such a cachexia. Thus, for example, 1-methylhistidine was found to be a putative marker in an NMR study of serum from individuals with hepatocellular carcinoma (Gao et al. 2009). This compound is a marker of muscle breakdown, and is present along with other amino acids in individuals with a range of cancers (Eisner et al. 2010). The elevated levels of 1-methylhistidine observed in our in vivo experiments may have been due to a combination of both tumor hypoxia and other metabolic changes in the host related to pain, anorexia, cachexia, etc.

Conclusions

By NMR metabolomics we have shown that there appears to be a hypoxia 'signature' evident in the serum from animals and in supernatants from cells grown under defined conditions. Identification of metabolite patterns that correspond to different tumor states (such as hypoxia) not only have the potential for being a clinically-relevant therapeutic or prognostic indicator, but may also point the way to metabolic pathways tumors require for their growth. As such, these would represent nodes for potential therapeutic intervention. For example, PDK-1 has a central role in lactate production and is indicative of poor prognosis in head and neck cancers (Wigfield et al. 2008). Inhibition of MCT1 leads to corresponding reduction of cancer growth (Sonveaux et al. 2008). The metabolite pattern presented herein may provide a tool for the detection of tumor hypoxia, a factor that may not only promotes tumor progression, but also acts limit the effectiveness of many types of anti-cancer treatments.

Acknowledgments The Metabolomics Research Centre at the University of Calgary is supported by funding from Alberta Health Services (AHS)/The Alberta Cancer Foundation (ACF). The studies were also supported in part by a translational grant from the AHS/ACF (to F.R.J.); F.R.J was the recipient of a Canada Research Chairs award.

References

Allen J, Davey H, Broadhurst D, Heald J, Rowland J, Oliver S, Kell D (2003) High-throughput classification of yeast mutants for functional genomics using metabolic footprinting. Nat Biotechnol 21:692–696

Bondareva A, Downey CM, Ayres F, Liu W, Boyd SK, Hallgrimsson B, Jirik FR (2009) The lysyl oxidase inhibitor, beta-aminopropionitrile, diminishes the metastatic colonization potential of circulating breast cancer cells. PLoS ONE 4:e5620

Chang D, Weljie AM, Newton J (2007) Leveraging latent information in NMR spectra for robust predictive models. Pac Symp Biocomput 12:115–126

Claudino WM, Quattrone A, Biganzoli L, Pestrin M, Bertini I, Di Leo A (2007) Metabolomics: available results, current research projects in breast cancer, and future applications. J Clin Oncol 25:2840–2846

DeBerardinis RJ, Lum JJ, Hatzivassiliou G, Thompson CB (2008) The biology of cancer: metabolic reprogramming fuels cell growth and proliferation. Cell Metab 7:11–20

Dowlatabadi R, Weljie AM, Thorpe TA, Yeung EC, Vogel HJ (2009) Metabolic footprinting study of white spruce somatic embryogenesis using NMR spectroscopy. Plant Physiol Biochem 47: 343–350

Eisner R, Stretch C, Eastman T, Xia J, Hau D (2010) Learning to predict cancer-associated skeletal muscle wasting from ^{1}H-NMR profiles of urinary metabolites. Metabolomics (in press)

Erler JT, Bennewith KL, Nicolau M, Dornhöfer N, Kong C, Le Q, Chi JA, Jeffrey SS, Giaccia AJ (2006) Lysyl oxidase is essential for hypoxia-induced metastasis. Nature 440:1222–1226

Gao H, Lu Q, Liu X, Cong H, Zhao L, Wang H, Lin D (2009) Application of ^{1}H NMR-based metabonomics in the study of metabolic profiling of human hepatocellular carcinoma and liver cirrhosis. Cancer Sci 100:782–785

Griffiths JR, McSheehy PM, Robinson SP, Troy H, Chung YL, Leek RD, Williams KJ, Stratford IJ, Harris AL, Stubbs M (2002) Metabolic changes detected by in vivo magnetic resonance studies of HEPA-1 wild-type tumors and tumors deficient in hypoxia-inducible factor-1beta (HIF-1beta): evidence of an anabolic role for the HIF-1 pathway. Cancer Res 62:688–695

Landaas S (1975) The formation of 2-hydroxybutyric acid in experimental animals. Clin Chim Acta 58:23–32

Lindon JC, Nicholson JK, Holmes E, Antti H et al (2003) Contemporary issues in toxicology the role of metabonomics in toxicology and its evaluation by the COMET project. Toxicol Appl Pharmacol 187:137–146

Perrin A, Roudier E, Duborjal H, Bachelet C, Riva-Lavieille C, Leverve X, Massarelli R (2002) Pyruvate reverses metabolic effects produced by hypoxia in glioma and hepatoma cell cultures. Biochimie 84:1003–1011

Schofield CJ, Ratcliffe PJ (2004) Oxygen sensing by HIF hydroxylases. Nat Rev Mol Cell Biol 5:343–354

Sonveaux P, Végran F, Schroeder T, Wergin MC et al (2008) Targeting lactate-fueled respiration selectively kills hypoxic tumor cells in mice. J Clin Invest 118:3930–3942

Ullah MS, Davies AJ, Halestrap AP (2006) The plasma membrane lactate transporter MCT4, but not MCT1, is up-regulated by hypoxia through a HIF-1alpha-dependent mechanism. J Biol Chem 281:9030–9037

Walenta S, Snyder S, Haroon ZA, Braun RD, Amin K, Brizel D, Mueller-Klieser W, Chance B, Dewhirst MW (2001) Tissue gradients of energy metabolites mirror oxygen tension gradients in a rat mammary carcinoma model. Int J Radiat Oncol Biol Phys 51:840–848

Warburg O (1956) On the origin of cancer cells. Science 123:309–314

Webb JD, Coleman ML, Pugh CW (2009) Hypoxia, hypoxia-inducible factors (HIF), HIF hydroxylases and oxygen sensing. Cell Mol Life Sci 66:3539–3554

Weljie A, Dowlatabadi R, Miller B, Vogel H, Jirik F (2007) An inflammatory arthritis-associated metabolite biomarker pattern revealed by ^{1}H NMR spectroscopy. J Proteome Res 6: 3456–3464

Weljie AM, Jirik FR (2010) Hypoxia-induced metabolic shifts in cancer cells: moving beyond the Warburg effect. Int J Biochem cell biol

Weljie AM, Newton J, Mercier P, Carlson E, Slupsky CM (2006) Targeted profiling: quantitative analysis of ^{1}H NMR metabolomics data. Anal Chem 78:4430–4442

Weljie AM, Newton J, Jirik FR, Vogel HJ (2008) Evaluating low-intensity unknown signals in quantitative proton NMR mixture analysis. Anal Chem 80:8956–8965

Wigfield SM, Winter SC, Giatromanolaki A, Taylor J, Koukourakis ML, Harris AL (2008) PDK-1 regulates lactate production in hypoxia and is associated with poor prognosis in head and neck squamous cancer. Br J Cancer 98:1975–1984

Wiklund S, Johansson E, Sjöström L, Mellerowicz EJ, Edlund U, Shockcor JP, Gottfries J, Moritz T, Trygg J (2008) Visualization of GC/TOF-MS-based metabolomics data for identification of biochemically interesting compounds using OPLS class models. Anal Chem 80:115–122

Wishart DS, Tzur D, Knox C, Eisner R et al (2007) HMDB: the Human Metabolome Database. Nucleic Acids Res 35:D521–D526

Wouters B, Koritzinsky M (2008) Hypoxia signalling through mTOR and the unfolded protein response in cancer. Nat Rev Cancer 8:851–864

Zhang H, Bosch-Marce M, Shimoda LA, Tan YS, Baek JH, Wesley JB, Gonzalez FJ, Semenza GL (2008) Mitochondrial autophagy is an HIF-1-dependent adaptive metabolic response to hypoxia. J Biol Chem 283:10892–10903